THE JOURNAL OF BIOLOGICAL CHEMISTRY VOL. 285, NO. 35, pp. 26976–26986, August 27, 2010
© 2010 by The American Society for Biochemistry and Molecular Biology, Inc. Printed in the U.S.A.

Na/H Exchanger Regulatory Factors Control Parathyroid Hormone Receptor Signaling by Facilitating Differential Activation of Gα Protein Subunits*

Received for publication, May 24, 2010, and in revised form, June 9, 2010 Published, JBC Papers in Press, June 18, 2010, DOI 10.1074/jbc.M110.147785

Bin Wang[‡], Juan A. Ardura[‡], Guillermo Romero[‡], Yanmei Yang[‡], Randy A. Hall[§], and Peter A. Friedman[‡1]

From the [‡]Laboratory for G Protein-coupled Receptor Biology, Department of Pharmacology and Chemical Biology, University of Pittsburgh School of Medicine, Pittsburgh, Pennsylvania 15261 and the [§]Department of Pharmacology, Emory University School of Medicine, Atlanta, Georgia 30322

The Na/H exchanger regulatory factors, NHERF1 and NHERF2, are adapter proteins involved in targeting and assembly of protein complexes. The parathyroid hormone receptor (PTHR) interacts with both NHERF1 and NHERF2. The NHERF proteins toggle PTHR signaling from predominantly activation of adenylyl cyclase in the absence of NHERF to principally stimulation of phospholipase C when the NHERF proteins are expressed. We hypothesized that this signaling switch occurs at the level of the G protein. We measured G protein activation by [^{35}S]GTPγS binding and Gα subtype-specific immunoprecipitation using three different cellular models of PTHR signaling. These studies revealed that PTHR interactions with NHERF1 enhance receptor-mediated stimulation of $G\alpha_q$ but have no effect on stimulation of $G\alpha_i$ or $G\alpha_s$. In contrast, PTHR associations with NHERF2 enhance receptor-mediated stimulation of both $G\alpha_q$ and $G\alpha_i$ but decrease stimulation of $G\alpha_s$. Consistent with these functional data, NHERF2 formed cellular complexes with both $G\alpha_q$ and $G\alpha_i$, whereas NHERF1 was found to interact only with $G\alpha_q$. These findings demonstrate that NHERF interactions regulate PTHR signaling at the level of G proteins and that NHERF1 and NHERF2 exhibit isotype-specific effects on G protein activation.

The parathyroid hormone receptor (PTHR)[2] is a Family B G protein-coupled receptor (GPCR) that regulates extracellular mineral ion homeostasis and bone growth and turnover. Interaction with its cognate ligands, PTH or the PTH-related peptide (PTHrP), stimulates adenylyl cyclase and phosphatidylinositol-specific phospholipase C (PLC) (1, 2). In some cases, occupancy of the PTHR activates only one signaling pathway. For example, in vascular smooth muscle cells, PTH stimulates adenylyl cyclase but not PLC (3, 4), whereas in keratinocytes (5, 6), cardiac myocytes (7, 8), and lymphocytes (9–11), the PTHR activates PLC but not adenylyl cyclase. In osteoblasts and kidney tubule cells, PTH activates both adenylyl cyclase and PLC (12–14). Occupancy of the PTHR activates multiple Gα proteins, and the physiologic responses to PTH may result from contributions of both α and βγ subunits. However, the particular G protein subunit to which the receptor couples varies in a cell-specific manner. Moreover, PTHR stimulation of PLC may arise through activation of G_q (4) or $G_{i/o}$ (15, 16).

The Na/H exchanger regulatory factor (NHERF) family consists of four related proteins as follows: NHERF1 and NHERF2 that contain two tandem PSD-95/Discs large/ZO-1 (PDZ) domains and an ezrin-binding domain, and NHERF3 and NHERF4 that possess four PDZ domains but no ezrin-binding domain (17). NHERF1 (also known as ezrin-binding phosphoprotein 50, EBP50) shares 52% amino acid identity with NHERF2, also called NHE3 kinase A regulatory protein (E3KARP) (18). NHERF1 and NHERF2 are implicated in protein targeting and in the assembly of protein complexes. They recruit various GPCRs, ion transporters, and other proteins to the plasma membrane of epithelia and other cells (19–22).

Despite the similarity between their PDZ domains, NHERF proteins exhibit different affinities for PDZ-binding partners. Some NHERF targets, like Taz (23), the PMCA2b Ca^{2+}-ATPase (24), and the LPA_5 receptor (25) preferentially bind NHERF2. Furthermore, NHERF2 may display distinct binding specificity and physiologic function that is not shared by NHERF1. NHERF2 but not NHERF1, for instance, specifically interacts with PLC-β3 and plays a key role in PLC-β3 activation by the PDZ domain-mediated interaction (26). Ca^{2+}-dependent inhibition of NHE3 requires an NHE3-NHERF2-α-actinin-4 complex for oligomerization and endocytosis (27). NHERF2 specifically interacts with the LPA_2 receptor and defines the specificity and efficiency of receptor-mediated PLC-β3 activation (28).

Mahon *et al.* (21) reported that NHERF2 inhibited adenylyl cyclase by stimulating inhibitory $G\alpha_i$ and increased PLC in PS120 cells transfected with the PTHR. In contrast, NHERF1 increased PTH-stimulated cAMP accumulation in ROS 17/2.8 cells (29). Adding to the variability of effects, both NHERF1 and NHERF2 increased PTH-stimulated PLC activity or intracellular calcium in PS120 cells, opossum kidney cells, and ROS 17/2.8 cells (21, 29–31), although no differences in PTH-stimulated cAMP formation were found in wild-type and NHERF1-

* This work was supported, in whole or in part, by National Institutes of Health Grants R01DK69998 (to P. A. F.) and R01NS055179 (to R. A. H.).
[1] To whom correspondence should be addressed: Dept. of Pharmacology and Chemical Biology, University of Pittsburgh School of Medicine, W-1340 Biomedical Science Tower, Pittsburgh, PA 15261. E-mail: paf10@pitt.edu.
[2] The abbreviations used are: PTHR, type 1 PTH receptor; PTH, parathyroid hormone; GPCR, G protein-coupled receptor; NHERF, Na/H exchange regulatory factor; PDZ, postsynaptic density 95/discs large/zona occludens; ROS, rat osteosarcoma; shRNA, short hairpin RNA; wtPTHR, wild-type PTHR; PLC, phospholipase C; PKC, protein kinase C; GTPγS, guanosine 5′-[γ-thio]-triphosphate; Ni-NTA, nickel-nitrilotriacetic acid; AMP-PCP, β,γ-methyleneadenosine 5′-triphosphate; res, rescue.

Downloaded from www.jbc.org at Emory University, on December 17, 2010

null proximal tubule cells (32, 33) or in CHO-N10-R3 cells in the presence or absence of NHERF1 (34).

The molecular mechanism by which NHERF association with PTHR promotes switching of receptor signaling between adenylyl cyclase and phospholipase C is not known. It has been speculated that the NHERF proteins may promote G_q-mediated signaling by tethering $G\alpha_q$ effectors such as PLC (26, 35), PKC (36), and PKD (37) in the vicinity of receptors. However, it is also possible that NHERF-GPCR interactions might directly modulate the G protein-coupling preferences of the receptors. The most direct and unambiguous way to determine the influence of NHERF1/2 on PTHR signaling is to measure effects on G protein activation. We show here that NHERF1 increases PTH-stimulated PTHR coupling to $G\alpha_q$ but not to $G\alpha_s$ or $G\alpha_i$. In contrast, NHERF2 decreases PTH-induced $G\alpha_s$ and increases $G\alpha_q$ and $G\alpha_i$ activation. These data reveal that NHERF-PTHR interactions can directly influence receptor coupling to G proteins.

EXPERIMENTAL PROCEDURES

HA.11 and His_6 monoclonal antibodies were obtained from Covance (Berkeley, CA). NHERF1 rabbit polyclonal antibody was purchased from Affinity Bioreagents (Golden, CO). NHERF2 rabbit polyclonal antibody was kindly provided by Dr. R. A. Frizzell (University of Pittsburgh). Polyclonal $G\alpha_s$ antibody was obtained from Millipore (Billerica, MA). $G\alpha_q$ monoclonal antibody was provided by BD Transduction Laboratories. $G\alpha_i$ polyclonal antibody was from NewEast Biosciences (Malvern, PA). Ni-NTA-agarose was provided by Qiagen (Valencia, CA). Horseradish peroxidase-conjugated goat anti-rabbit secondary antibody was from Pierce. Horseradish peroxidase-conjugated sheep anti-mouse antibody was from GE Healthcare. Lipofectamine 2000 and geneticin, protein A-Sepharose 4B conjugate, and rec-protein G-Sepharose 4B conjugate were obtained from Invitrogen. Protease inhibitor mixture Set I and pertussis toxin were from Calbiochem. Human PTH(1–34) was purchased from Bachem (Torrance, CA). $[^{35}S]GTP\gamma S$ (1,250 Ci/mmol) was purchased from PerkinElmer Life Sciences. FuGENE 6 was purchased from Roche Applied Science. All other reagents were from Sigma.

Cell Culture—PS120 cells were stably transfected with PTHR (PS120-R) or stably transfected with both PTHR and NHERF2 (PS120-R-N2) and were obtained from Dr. M. J. Mahon (Harvard Medical School). PS120-R cells were cultured in Dulbecco's modified Eagle's medium with 10% fetal bovine serum, 100 units/ml penicillin, 100 μg/ml streptomycin, 1 μg/ml puromycin. PS120-R-N2 cells were cultured in the above medium with additional 0.1 mg/ml hygromycin B. CHO cells were stably transfected with PTHR (CHO-R) (34) and cultured in Ham's F-12 medium supplemented with 10% fetal bovine serum, 100 units/ml penicillin, 100 μg/ml streptomycin, and 0.75 mg/ml geneticin. HEK-293 cells were stably transfected with PTHR (HEK-293R) (34) and cultured in Dulbecco's modified Eagle's medium/F-12 medium supplemented with 10% fetal bovine serum, 100 units/ml penicillin, 100 μg/ml streptomycin, and 0.75 mg/ml geneticin. All cells were maintained at 37 °C in a humidified atmosphere of 5% CO_2, 95% air.

Transient Transfection—Cells were transiently transfected with empty vector, plasmids of His-NHERF1 (34), His-NHERF2 (provided by Dr. R. A. Frizzell, University of Pittsburgh), wild-type PTH receptor (PTHR-ETVM), mutant PTHR (PTHR-ETVA) (34), $^{YFP}G\alpha_i$ (provided by Dr. J.-P. Vilardaga, University of Pittsburgh), bimolecular fluorescence complementation $\beta_1\gamma_2$ complexes (provided by Dr. C.H. Berlot) (38), as indicated, using FuGENE 6 or Lipofectamine 2000 as described previously (39). Cells were used 48 h after transfection.

Membrane Preparation—Plasma membranes were isolated by differential centrifugation at 4 °C as described previously (1, 39, 40). Briefly, after cells achieved confluence, they were rinsed with cold PBS and then incubated with hypotonic buffer (10 mM Hepes, 0.5 mM EDTA, pH 7.4) for 15 min. Swollen cells were harvested, collected by centrifugation (1000 × *g* for 10 min), and resuspended in ~9 volumes of 10 mM Tris, 1 mM EDTA, pH 7.4, with proteinase inhibitor mixture set I. Cells were disrupted with 20–40 strokes in a "loose" Dounce homogenizer on ice. The lysates were centrifuged at 1000 × *g* for 10 min to remove unbroken cells, large cell debris, and some nuclei. The supernatant was further centrifuged at 30,000 × *g* for 20 min. The membrane pellet was resuspended in freezing buffer (10 mM Hepes, 0.1 mM EDTA, pH 7.4) at a protein concentration of 5–10 μg/μl and rapidly frozen in liquid nitrogen. Membranes were then stored at −80 °C until used.

GTPγS Binding and Immunoprecipitation of GTPγS-bound Gα Subunits—The comparative changes in $G\alpha$-$[^{35}S]GTP\gamma S$ binding immunoprecipitated by specific Gα subtype-specific antisera were used to delineate PTHR coupling to distinct Gα protein subunits. $[^{35}S]GTP\gamma S$ binding to G proteins was performed with a modification of previously described methodologies (1, 40). Frozen membrane aliquots (150 μg) were incubated with 100 μl of assay buffer (10 mM Hepes, 100 mM NaCl, 5 mM $MgCl_2$, pH 7.4) containing 5 μM GDP, 5 nM $[^{35}S]GTP\gamma S$, and 100 nM PTH(1–34) at 30 °C for 5 min (unless otherwise stated). Incubations were terminated by the addition of 800 μl of ice-cold assay buffer and immediate transfer to an ice bath. Cell membranes were recovered from the reaction mixture by centrifugation at 20,000 × *g* for 10 min, and the resulting supernatant was removed. Membrane pellets were solubilized, and immunoprecipitation of $[^{35}S]GTP\gamma S$ bound to Gα subunits was measured as described below under "Coimmunoprecipitation and Immunoblot Analysis." After Sepharose beads were washed three times, the beads were resuspended with 100 μl of 0.5% SDS and incubated at 85–90 °C for 2–3 min. The entire contents of each tube were transferred to a vial containing 5 ml of scintillation mixture, and radioactivity was measured by β-emission spectrometry. Nonspecific binding was determined in the presence of 100 μM GTPγS.

Coimmunoprecipitation and Immunoblot Analysis—Interaction of G proteins with NHERF1 or NHERF2 was analyzed as described previously (41). In brief, 6-well plates of CHO-R3 cells were transiently transfected with His-NHERF1, His-NHERF2, or empty vector. Forty eight hours later, the cells were lysed with 1% Lubrol, 0.5% sodium deoxycholate, 0.1% SDS, 50 mM Tris, pH 7.4, and 150 mM NaCl. Solubilized materials were incubated overnight at 4 °C with Ni-NTA-agarose or

Downloaded from www.jbc.org at Emory University, on December 17, 2010

TABLE 1

Primers used to generate rescue forms of human NHERF1 and NHERF2

Three silent mutations (underlined) were introduced in the shRNAs targeting NHERF1 or NHERF2.

	Gene sequences
NHERF1 sense	5′-CTGGTGGTGGACAGGGA<u>G</u>AC<u>C</u>GA<u>T</u>GAGTTCTTCAAGAAATGC
NHERF1 antisense	5′-GCATTTCTTGAAGAACTC<u>A</u>TC<u>G</u>GT<u>C</u>TCCCTGTCCACCACCAG
NHERF2 sense	5′-CAGATGGACTGGAACAG<u>A</u>AA<u>A</u>CG<u>C</u>GAAATCTTCAGCAAC
NHERF2 antisense	5′-GTTGCTGAAGATTTC<u>G</u>CG<u>T</u>TT<u>T</u>CTGTTCCAGTCCATCTG

incubated with anti-Gα_s polyclonal antibody, Gα_q monoclonal antibodies, or Gα_i polyclonal antibody for 1 h at 4 °C and then protein A or protein G-Sepharose 4B conjugate was added to each sample and incubated overnight at 4 °C. Total lysates and immunoprecipitated protein, eluted by the addition of SDS sample buffer, were analyzed by SDS-polyacrylamide gels and transferred to Immobilon-P membranes (Millipore) using the semi-dry method (Bio-Rad). Membranes were blocked overnight at 4 °C with 5% nonfat dried milk in Tris-buffered saline plus Tween 20 and incubated with different antibodies (anti-His antibody (1:1000); anti-Gα_s (1:500); anti-Gα_q (1:250); anti-Gα_i (1:500); anti-HA (1:1000); anti-NHERF1 (1:1000); anti-NHERF2 (1:4000); or anti-actin (1:2000)) for 2 h at room temperature. The membranes were then washed and incubated with goat anti-rabbit IgG conjugated to horseradish peroxidase or anti-sheep mouse IgG conjugated to horseradish peroxidase (1:5000) for 1 h at room temperature. Protein bands were revealed with a luminol-based enhanced chemiluminescence substrate.

Overlay Assay—His/S-tagged PDZ1 and PDZ2 domain proteins (1 μg/lane) were spotted on nylon membrane as described previously (42). The membranes were blocked with blot buffer for 30 min at room temperature and then overlaid with 100 nM GST-tagged C-terminal 22-amino acid fragments of wild-type PTHR (PTHR-ctETVM) or its mutant form PTHR-ctETVA in blot buffer for 1 h at room temperature. The blots were washed and incubated with horseradish peroxidase-conjugated anti-GST antibody (1:3000). Interactions of the GST fusion proteins with the PDZ domains were visualized by chemiluminescence.

NHERF Knockdown—Constitutive NHERF1 or NHERF2 expression in HEK-293R cells was silenced using RNA interference. Short hairpin RNA (shRNA) constructs against human NHERF1 (GGAAACTGACGAGTTCTTCAAGAAATGCA) and NHERF2 (AACAGGAAGCGTGAAATCTTCAGCAACTT) were purchased from OriGene (Rockville, MD). HEK-293R cells were transfected with NHERF1 shRNA, NHERF2 shRNA, or scrambled shRNA. Transfections were established and described previously (34). Transfected cells were cultured for 72 h and then used for G protein binding or immunoblot.

Rescue forms of human NHERF1 and NHERF2 (resNHERF1 and resNHERF2, respectively) resistant to their respective shRNA were generated by introducing three silent mutations in the NHERF1 and NHERF2 sequences using primers listed in Table 1. The mutations were constructed by PCR using the QuikChange site-directed mutagenesis kit (Stratagene, La Jolla, CA) according to the manufacturer's instructions. The fidelity of plasmids was confirmed by sequencing (ABI PRISM 377, Applied Biosystems, Foster City, CA). Rescue shRNA scrambled constructs containing the 29-mer scrambled cassette were purchased from OriGene.

FRET—Gα_i activation was measured in real time in live cells by fluorescence resonance energy transfer (FRET) as described previously (43, 44). Briefly, HEK-293 cells plated on MatTek (Ashland, MA) dishes were maintained in Hepes buffer with 0.1% (w/v) bovine serum albumin at 22 °C. Cells were observed using a 40 × 1.30 NA oil immersion objective on a Nikon A1s confocal microscope attached to a Ti-E inverted base. Subunit rearrangement of Gα_i and G$\beta\gamma$ was measured by FRET between YFP-tagged Gα_i and cerulean-tagged G$\beta_1\gamma_2$ bimolecular fluorescence complementation. FRET signal was measured as the normalized FRET ratio (nFRET) of the YFP and cyan fluorescent protein emission (F_{YFP}/F_{CFP}) (45).

Receptor Binding—Receptor binding was performed as described previously (34) using HPLC-purified ^{125}I-[Nle^{8,18},Tyr^{34}]PTH(1–34)-NH_2. In brief, PS120-R cells, PS120-R-N2, or CHO-R3 cells were seeded on 24-well plates and grown to confluence. Cells were put on ice for 15 min and incubated with PTH(1–34) (10^{-11}–10^{-6} M) and ~100,000 cpm of ^{125}I-[Nle^{8,18},Tyr^{34}]PTH(1–34)-NH_2 in 250 μl of fresh media on ice for an additional 2.5 h. After incubation, cells were rinsed twice with ice-cold PBS and then solubilized in 0.2 N NaOH. Nonspecific binding was measured in parallel experiments carried out in the presence of 1 μM unlabeled PTH(1–34). Cell surface-bound ^{125}I-PTH(1–34) was assessed by γ-spectrometry. PTHR number was analyzed by Scatchard analysis.

Adenylyl Cyclase—Adenylyl cyclase activity was determined by assay of cAMP accumulation as described previously (34). Briefly, HEK-293R cells transfected with scrambled shRNA, NHERF1 shRNA, or NHERF2 shRNA in 24-well plates were labeled with 0.5 μCi of [^{3}H]adenine for 2 h. The cells were then treated with vehicle or 100 nM PTH(1–34) in the presence of phosphodiesterase inhibitor 3-isobutyl-1-methylxanthine (1 mM) for 15 min. The reaction was terminated by addition of 1 M TCA. cAMP was isolated by the two-column method.

Intracellular Calcium—Intracellular calcium concentrations ($[Ca^{2+}]_i$) were measured with the calcium-sensitive dye Fluo-4/AM (Invitrogen) following the manufacturer's protocol. Briefly, HEK-293R cells were cultured on MatTek dishes with 2 μM Fluo-4/AM in Hanks' balanced salt solution (Invitrogen) at 22 °C for 45 min. Cells were washed three times with Hanks' balanced salt solution and incubated with Hanks' balanced salt solution at 22 °C for another 30 min. The calcium measurements were performed with a Nikon A1s inverted fluorescent microscope. Fluorescence was recorded at 1-s intervals for up to 20 min. At least 30–40 cells were counted under each condition. Intracellular calcium concentrations were calculated using the following equation: $[Ca^{2+}]_i = K_d \times (F - F_{min})/(F_{max} - F)$, where F is the measured fluorescence intensity; F_{max} is the fluorescence measured after addition of 10 μM ionomycin; F_{min} is the fluorescence measured after addition of 10 mM EGTA, and K_d is the dissociation constant of the dye-Ca^{2+} complex (520 nM) (46).

Statistics—Data are presented as the mean ± S.E., where n indicates the number of independent experiments. Multiple

Downloaded from www.jbc.org at Emory University, on December 17, 2010

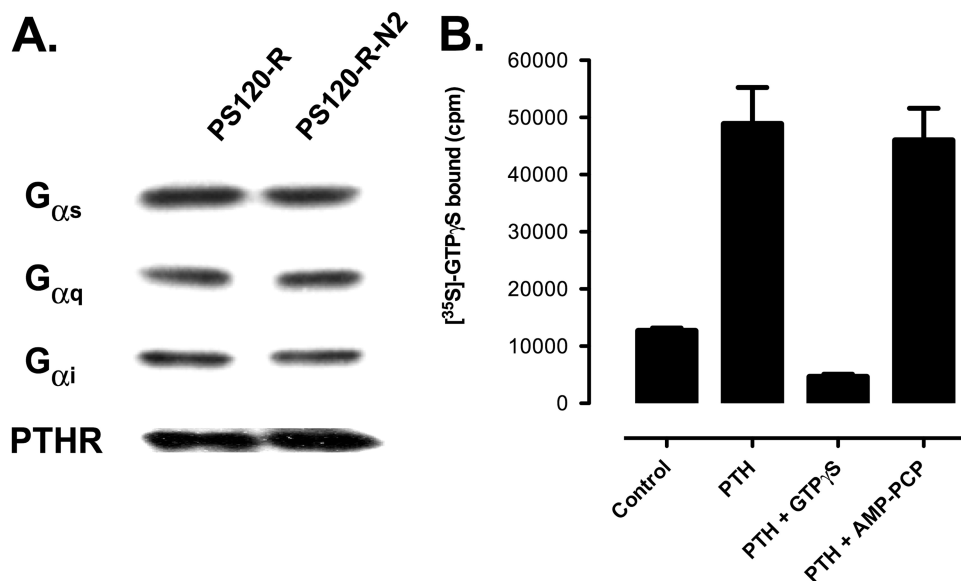

FIGURE 1. **Specificity of PTH-induced [^{35}S]GTPγS binding to G protein subunit.** *A*, cell membrane protein (20 μg) prepared from PS120-R or PS120-R-N2 cells was resolved on 10% SDS-polyacrylamide gels as described under "Experimental Procedures" for immunoblot analysis. Cell membrane PTHR expression was used as a loading control (55). *B*, membrane aliquots from PS120-R cells were incubated with [^{35}S]GTPγS and 100 nM PTH(1–34) in the presence or absence of 1 mM AMP-PCP or 100 μM unlabeled GTPγS for 5 min at 30 °C. Immunoprecipitation of [^{35}S]GTPγS bound to Gα_s subunit was measured as described under "Experimental Procedures." Data are summarized as the mean ± S.E. of three independent experiments.

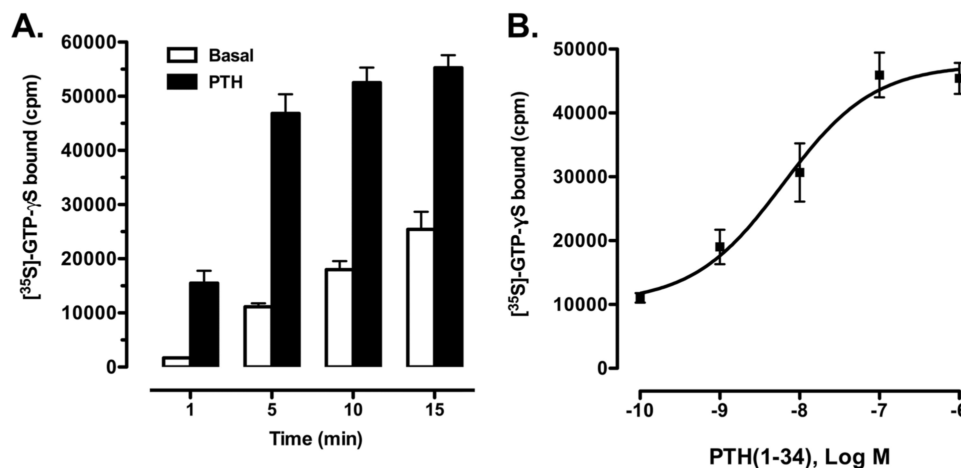

FIGURE 2. **Time- and concentration-dependent PTH induction of [^{35}S]GTPγS binding to Gα_s protein subunit.** Cell membranes were prepared from PS120-R cells. Data are summarized as the mean ± S.E. of three independent experiments. *A*, time course of PTH-stimulated [^{35}S]GTPγs binding to Gα_s subunit was measured in the presence or absence of 100 nM PTH(1–34). *B*, concentration-dependent curve of PTH-stimulated [^{35}S]GTPγs binding to Gα_s subunit was measured in the presence of PTH for 5 min. Data are summarized as the mean ± S.E. of three independent experiments.

comparisons were evaluated by analysis of variance with post-test repeated measures analyzed by the Duncan procedure using Prism (GraphPad Software, Inc., San Diego). Differences of $p < 0.05$ were assumed to be significant.

RESULTS

Specificity of PTH-induced Gα Subunit Activation—We first determined the constitutive expression of Gα protein subunits in membranes of PS120-R cells. Fig. 1*A* shows that PS120-R cells express Gα_s, Gα_q, and Gα_i proteins in cell membranes. We then measured PTH-stimulated [^{35}S]GTPγS binding to Gα_s, Gα_q, and Gα_i. PTH increased [^{35}S]GTPγS binding to Gα_s protein by 3.6-fold (Fig. 1*B*). Unlabeled GTPγS (100 μM) virtually abolished PTH-induced [^{35}S]GTPγS binding. The nonhydrolyzable ATP analogue AMP-PCP (1 mM) had no effect on PTH-induced [^{35}S]GTPγS binding. Similar results obtained with PTH-stimulated [^{35}S]GTPγS binding to Gα_q and Gα_i (data not shown). These data provide strong evidence for specificity of PTH-induced [^{35}S]GTPγS binding to Gα_s, Gα_q, and Gα_i proteins.

PTH activated Gα_s in a time- and concentration-dependent manner. Ligand-stimulated [^{35}S]GTPγS binding to Gα_s occurred within 1 min (Fig. 2*A*). Because Gα-[^{35}S]GTPγS is resistant to hydrolysis by the intrinsic GTPase activity of Gα, [^{35}S]GTPγS-labeled Gα subunits accumulated over time under both basal and PTH-stimulated conditions. The net change of PTH-stimulated [^{35}S]GTPγS binding peaked at 5 min. Therefore, we used this time point to determine the concentration dependence of PTH action. Half-maximal PTH-induced [^{35}S]GTPγS binding was 6.2 nM; maximal stimulation occurred at 100 nM (Fig. 2*B*). Similar results were observed for PTH-stimulated [^{35}S]GTPγS binding to Gα_q and Gα_i (data not shown). Therefore, 5 min stimulations with 100 nM PTH were used for subsequent experiments.

NHERF2 Inhibits PTH-stimulated Gα_s and Increases Gα_q and Gα_i Activation—Mahon *et al.* (21) reported that NHERF2 switched PTHR signaling from adenylyl cyclase to PLC in PS120-R cells stably transfected with NHERF2 (PS120-R-N2). Pertussis toxin pretreatment of PS120-R-N2 cells markedly inhibited PTH activation of PLC and enhanced activation of adenylyl cyclase, implying that PTH stimulates $G_{i/o}$ proteins when the PTHR is bound to NHERF2. We tested the effects of NHERF2 on resting and PTH-stimulated Gα_s, Gα_q, and Gα_i exchange. PS120-R cells express small amounts of NHERF1 (47) but not NHERF2 (Fig. 3*A*), whereas PS120-R-N2 cells express NHERF2 mostly at cell membranes (Fig. 3*A*). NHERF2 did not affect basal Gα_s, Gα_q, or Gα_i activity but significantly blunted PTH-stimulated Gα_s activation (Fig. 3*B*). Conversely, NHERF2 augmented Gα_q and Gα_i activation (Fig. 3*B*). These effects occurred without a detectable change in cell membrane PTH receptor abundance (Fig. 3*C*), suggesting that the action of NHERF2 on Gα GTP exchange is not due to altered abundance of the PTHR or of ligand binding to the PTHR.

Downloaded from www.jbc.org at Emory University, on December 17, 2010

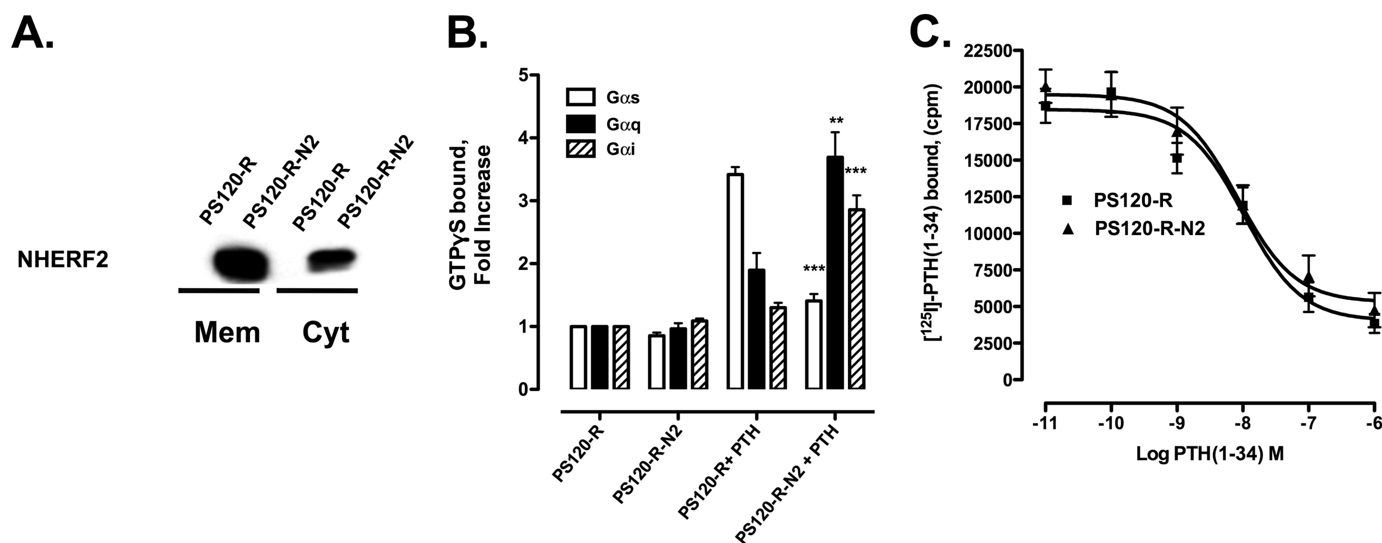

FIGURE 3. **NHERF2 inhibits PTH-stimulated $G\alpha_s$ binding and increases both $G\alpha_q$ and $G\alpha_i$ binding in PS120-R cell membranes.** *A*, equal amounts of membrane (*Mem*) and cytosolic (*Cyt*) proteins (20 μg) from PS120-R cells or PS120-R-N2 cells were immunoblotted with NHERF2 antibody. *B*, PTH-stimulated [^{35}S]GTPγs binding to $G\alpha_s$, $G\alpha_q$, or $G\alpha_i$ protein was measured in PS120-R or PS120-R-N2 cell membranes. Data are summarized as the mean ± S.E. of four independent experiments. **, $p < 0.01$; ***, $p < 0.001$, compared with PS120-R plus PTH group. *C*, cell surface binding of ^{125}I-PTH(1–34) in PS120-R cells or PS120-R-N2 cells was measured as described under "Experimental Procedures." Data are summarized as the mean ± S.E. of triplicate determinations.

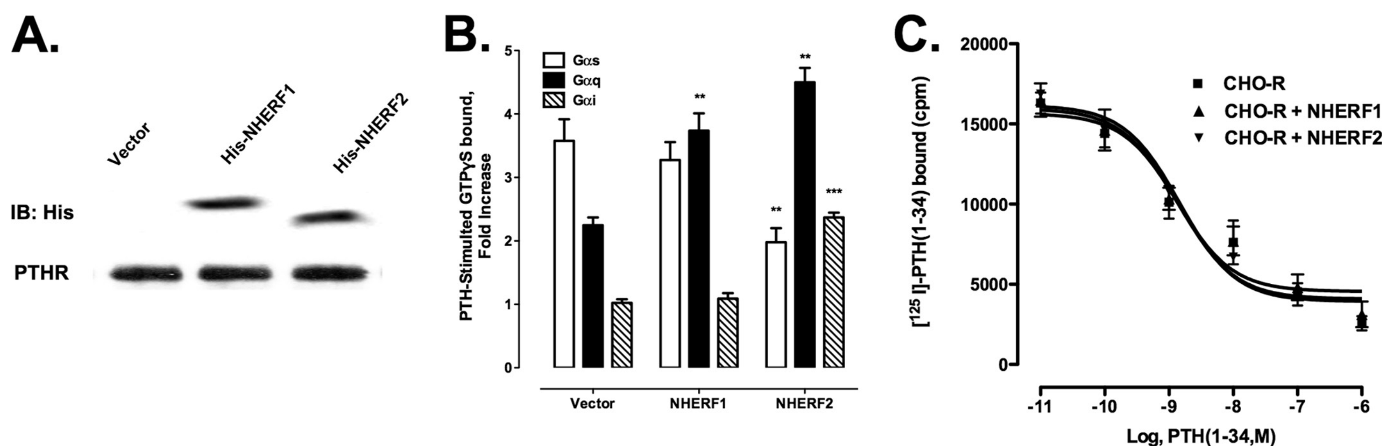

FIGURE 4. **Effects of NHERF1 and NHERF2 on PTH-stimulated [^{35}S]GTPγS binding to $G\alpha$ protein subunits in CHO-R cell membranes.** *A*, equal amounts of membrane proteins (20 μg) from CHO-R cells transiently transfected with vector, His-NHERF1, or His-NHERF2 were immunoblotted (*IB*) with His antibody. Cell membrane PTHR expression was used as a loading control. *B*, PTH-stimulated [^{35}S]GTPγs binding to $G\alpha_s$, $G\alpha_q$, or $G\alpha_i$ protein was measured in the cell membranes of CHO-R cells transiently transfected with vector, His-NHERF1, or His-NHERF2. Data are summarized as the mean ± S.E. of four independent experiments. **, $p < 0.01$; ***, $p < 0.001$ compared with vector plus PTH group. *C*, cell surface binding of ^{125}I-PTH(1–34) in CHO-R cells transiently transfected with vector, His-NHERF1, or His-NHERF2 was measured. Data are summarized as the mean ± S.E. of triplicate determinations.

Downloaded from www.jbc.org at Emory University, on December 17, 2010

NHERF1 and NHERF2 Differentially Regulate PTH-stimulated Gα Activation—The ability of PTH to increase the coupling of the receptor to $G\alpha_s$ and $G\alpha_q$ correlates with ligand-induced, receptor-dependent sensitivity of adenylyl cyclase and PLC signaling (1). Based on the described differences of NHERF1 and NHERF2 regulation of PTHR signaling (21, 29, 34), we hypothesized that NHERF1 and NHERF2 might differentially regulate PTH-stimulated Gα protein activation. To compare the effects of NHERF1 and NHERF2 on G_s activation, we used CHO cells stably transfected with PTHR (CHO-R), which lack detectable expression of NHERF1 (34) or NHERF2 (data not shown) but express similar levels of $G\alpha_s$, $G\alpha_q$, and $G\alpha_i$ proteins (40). We transiently transfected CHO-R cells with His-NHERF1 or His-NHERF2, resulting in similar levels of cell membrane expression (Fig. 4*A*). In the absence of NHERF1 or NHERF2, PTH activation of $G\alpha_s$ was greater than that of $G\alpha_q$, but no effects on $G\alpha_i$ activation were detected (Fig. 4*B*). Neither NHERF1 nor NHERF2 affected basal Gα activity (data not shown). In the presence of NHERF1, PTH significantly enhanced $G\alpha_q$ activity without an effect on $G\alpha_s$ or $G\alpha_i$ (Fig. 4*B*). Thus, NHERF1 selectively promotes receptor coupling to $G\alpha_q$. In contrast, NHERF2 significantly inhibited PTH-stimulated $G\alpha_s$ but enhanced PTH-induced activation of $G\alpha_q$ and $G\alpha_i$ (Fig. 4*B*). NHERF2 therefore influences receptor coupling to all three G_α proteins, promoting opposite effects on $G\alpha_s$ and $G\alpha_i$, but like NHERF1 increasing PTH-dependent $G\alpha_q$ activity. NHERF1 and NHERF2 did not affect receptor number as evidenced by comparable PTH binding to the PTHR (Fig. 4*C*), consistent with previous reports on CHO and ROS 17/2.8 cells (29, 34).

The PTHR, through its C-terminal ETVM PDZ recognition sequence, interacts with NHERF1 by binding to PDZ1 and

PDZ2 (34, 48). PTHR interactions with NHERF2 PDZ domains have not been described. Here, we simultaneously compared the interactions of GST-tagged C-terminal 22 amino acid peptide fragments of the wild-type PTHR (PTHR-ctETVM) and a mutant form PTHR-ctETVA, which cannot bind NHERF1, with PDZ1 and PDZ2 domains of NHERF1 and NHERF2 (Fig. 5*A*). The results show that the PTHR preferentially interacts with the PDZ1 domain of NHERF1 and PDZ2 of NHERF2. These associations were abolished with the PTHR harboring the mutated PDZ interaction motif.

Additional examination of the NHERF-mediated switch of G protein activation was undertaken in HEK-293 cells, which constitutively express NHERF1 and NHERF2. In HEK-293 cells, transfected with wild-type PTHR-ETVM (Fig. 5*B*), PTH significantly activated $G\alpha_s$, $G\alpha_q$, and $G\alpha_i$ (Fig. 5*C*), consistent with a previous report that PTH promoted activation of $G\alpha_s$, $G\alpha_{q/11}$, and $G\alpha_i$ in HEK-293 cells (1). The PTHR-ETVA, which does not bind NHERF (49), showed decreased PTH-stimulated $G\alpha_q$ activation and increased PTH-stimulated activation of $G\alpha_s$ (Fig. 5*C*), although $G\alpha_i$ activation was absent. To delineate the individual effects of NHERF1 and NHERF2 on G protein activation, endogenous NHERF1 or NHERF2 expression was silenced by RNA interference. A scrambled shRNA was used as a control. NHERF1 or NHERF2 shRNA reduced endogenous NHERF1 or NHERF2 levels by 78 and 82%, respectively, compared with a scrambled control (Fig. 5*D*). NHERF1 shRNA did not interfere with NHERF2 expression, and conversely, NHERF2 shRNA did not affect NHERF1 expression, demonstrating the specificity of the knockdown of endogenous NHERF1 and NHERF2 by their respective shRNAs. Neither shRNA affected basal [^{35}S]GTPγS binding to Gα subunits (data not shown). Knockdown of NHERF1 expression selectively inhibited PTH-stimulated activation of $G\alpha_q$ (Fig. 5*E*). Silencing NHERF2 expression, in contrast, significantly increased PTH-stimulated $G\alpha_s$ and inhibited $G\alpha_i$ activation. To rule out off-target effects of shRNA, we generated NHERF1 and NHERF2 rescue constructs (resNHERF1 and resNHERF2) harboring silent mutations to their respective shRNA and then conducted rescue experiments in HEK-293R cells. Expression of resNHERF1 blocked shNHERF1 inhibition of PTH-stimulated activation of $G\alpha_q$ (Fig. 5*F*). resNHERF2 abolished shNHERF2 increases of PTH-stimulated $G\alpha_s$ and inhibition of $G\alpha_i$ activation.

Further and independent characterization of the dynamic interactions of NHERF1 and NHERF2 with $G\alpha_i$ was conducted using real time FRET in living cells. PTH activated $G\alpha_i$ in HEK-293 cells transfected with PTHR-ETVM compared with the cells transfected with PTHR-ETVA (Fig. 5*G*). NHERF1 shRNA did not affect PTH-induced $G\alpha_i$, whereas the FRET signal was abolished with shNHERF2. These data further confirm that NHERF2 specifically increases PTH-induced $G\alpha_i$ activation. Taken together, these results provide a mirror image of the effects of individual NHERF1 and NHERF2 actions on CHO-R cells and show that NHERF1 augments receptor-mediated stimulation of $G\alpha_q$ but has no effect on stimulation of $G\alpha_i$ or $G\alpha_s$, whereas NHERF2 enhances receptor-mediated stimulation of both $G\alpha_q$ and $G\alpha_i$ but decreases stimulation of $G\alpha_s$.

NHERF2 but Not NHERF1 Binds $G\alpha_i$ and Regulates Second Messenger Signaling Pathways—NHERF1 interacts directly with $G\alpha_q$ (35). We analyzed NHERF1 and NHERF2 binding to $G\alpha_s$, $G\alpha_q$, and $G\alpha_i$. CHO-R cells were transiently transfected with His-NHERF1 or His-NHERF2. Neither NHERF1 nor NHERF2 interacted with $G\alpha_s$ (data not shown). However, both NHERF1 and NHERF2 bound $G\alpha_q$, and the interactions were enhanced in the presence of PTH (Fig. 6*A*). These data are consistent with the report that NHERF1 interacts with $G\alpha_q$ and to a greater extent with $G\alpha_q$-R183C, a constitutively active $G\alpha_q$ mutant (35). We next investigated the interaction of NHERF1 and NHERF2 with $G\alpha_i$. NHERF2 but not NHERF1 coimmunoprecipitated with $G\alpha_i$ by using Ni-NTA-agarose followed by immunodetection with a $G\alpha_i$ antibody (Fig. 6*B*). Likewise, the interaction could be detected by using a $G\alpha_i$ antibody for immunoprecipitation and immunodetection of NHERF2 with a His antibody. The association was also enhanced in the presence of PTH (Fig. 6*B*). Importantly, NHERF2 interacted with endogenous $G\alpha_i$ in native CHO cells not expressing the PTHR (Fig. 6*C*), indicating that the interaction between NHERF2 and $G\alpha_i$ is receptor-independent.

Since NHERF1 and NHERF2 differentially regulate PTH-stimulated $G\alpha_i$ activation, their effects on PTH-induced second messenger signaling pathways in the presence or absence of pertussis toxin should differ. Therefore, we examined the effect of NHERF1 or NHERF2 on PTH-stimulated cAMP formation and $[Ca^{2+}]_i$, as an index of PLC activity, in HEK-293R cells. Pertussis toxin (100 ng/ml) pretreatment for 16 h markedly increased PTH activation of adenylyl cyclase (Fig. 7*A*), without affecting the magnitude of PTH-induced $[Ca^{2+}]_i$ (Fig. 7*B, top*), consistent with a previous report regarding pertussis toxin effects on PTH-stimulated cAMP formation and $[Ca^{2+}]_i$ (15). Silencing NHERF1 did not affect PTH-stimulated cAMP formation or maximal $[Ca^{2+}]_i$. Pertussis toxin increased PTH-stimulated cAMP accumulation and decreased $[Ca^{2+}]_i$ in the presence of shNHERF1 (Fig. 7, *A* and *B, middle*). As expected, pertussis toxin had no further action on PTH-stimulated cAMP production or $[Ca^{2+}]_i$ after knockdown of NHERF2 (Fig. 7, *A* and *B, bottom*). Taken together, these results show that NHERF1 and NHERF2 differentially regulate PTH-stimulated G protein activation and second messenger signaling pathways.

DISCUSSION

PTH activates multiple second messenger signaling pathways that are reportedly coupled by distinct G proteins to the PTHR. Indirect approaches suggest that the PTHR is capable of coupling to $G\alpha_s$ and to multiple $G\alpha_q$ family members (2) and $G\beta\gamma$ subunits (50). However, to the best of our knowledge, only a single report analyzed PTHR activation of G proteins (1). Schwindinger *et al.* (1) measured PTHR coupling to Gα proteins in HEK-293 cell lines heterologously expressing the PTHR at low (C20; 40,000 receptors/cell) or high (C21; 400,000 receptors/cell) and in ROS 17/2.8 osteosarcoma cells, which constitutively express 72,000 receptors/cell (51). The ability of PTH(1–34) to activate $G\alpha_s$ and $G\alpha_q$, measured by [α-^{32}P]GTP-γ-azidoanilide binding followed by immunospecific Gα subunit detection, correlated with the magnitude of ligand-induced receptor-dependent

Downloaded from www.jbc.org at Emory University, on December 17, 2010

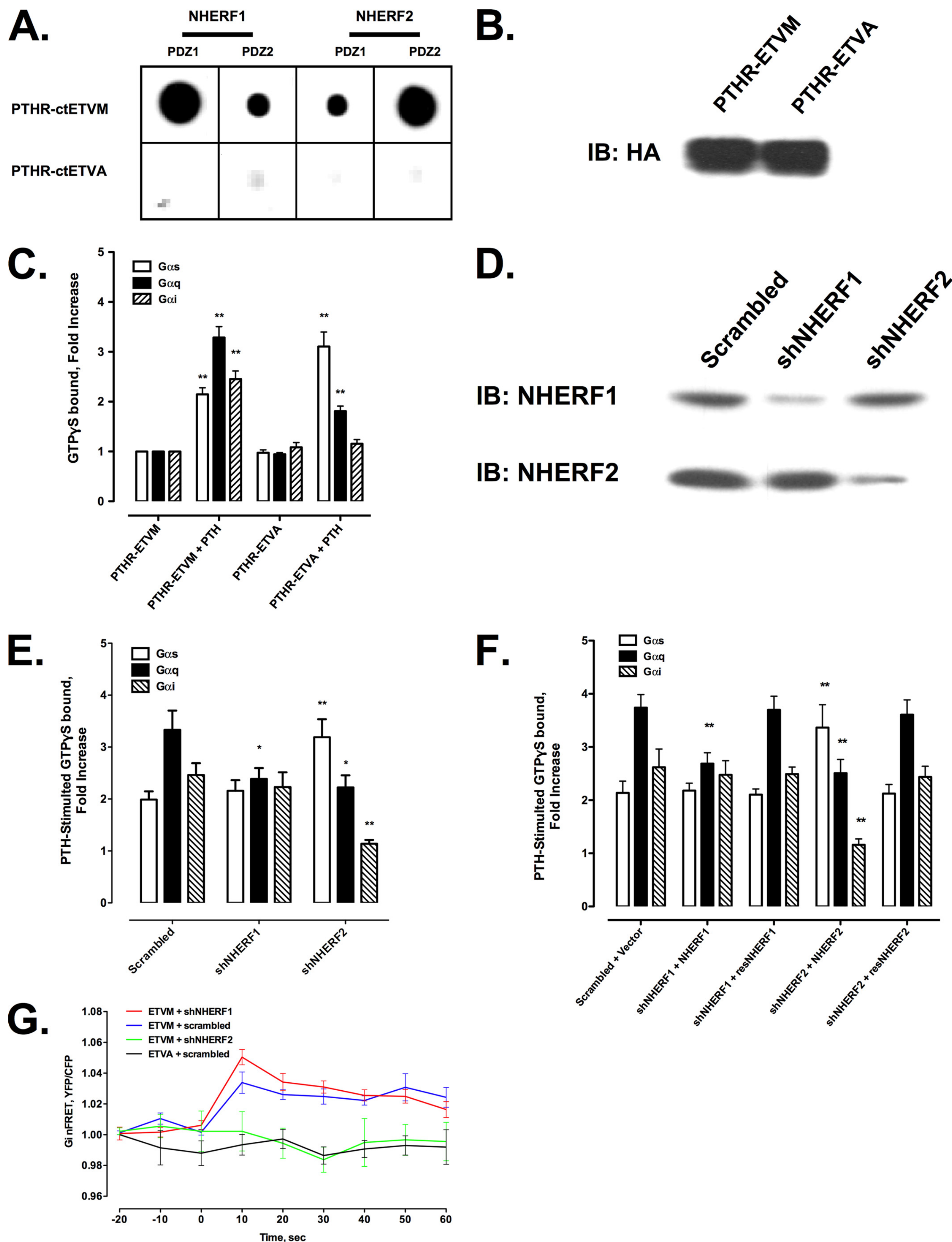

Downloaded from www.jbc.org at Emory University, on December 17, 2010

FIGURE 6. **NHERF2 but not NHERF1 binds $G\alpha_i$.** *A*, PTH increased the interaction of $G\alpha_q$ protein with NHERF1 or NHERF2. CHO-R cells were transfected with His-NHERF1 or His-NHERF2. His-tagged proteins were precipitated with Ni-NTA-agarose. The precipitated protein was then immunoblotted (*IB*) with $G\alpha_q$ antibody. *B*, PTH increased the interaction of $G\alpha_i$ proteins with NHERF2. CHO-R cells were transfected with His-NHERF1 or His-NHERF2. His-tagged proteins were precipitated with Ni-NTA-agarose or endogenous $G\alpha_i$ protein was precipitated with $G\alpha_i$ antibody. The precipitated proteins were immunoblotted with either $G\alpha_i$ or His antibody. *C*, interaction of $G\alpha_q$ or $G\alpha_i$ subunits with NHERF1 or NHERF2 in CHO cells was measured and described as above. Data are representative of three independent experiments. *IP*, immunoprecipitated.

sensitivity of adenylyl cyclase and PLC signaling pathways. PTH promoted activation of $G\alpha_s$, $G\alpha_{q/11}$, and $G\alpha_i$, albeit to a lesser extent, in C21 but not in C20 cells. In ROS 17/2.8 cells, PTH activated $G\alpha_s$ to a greater degree than in C21 cells but had no effect on $G\alpha_{q/11}$ or $G\alpha_i$. NHERF proteins had not been discovered that at the time those studies were performed. Our data now permit some comparison of the results and show that the expression of NHERF1 and NHERF2 are, at least in part, responsible for the heterogeneity of the cellular responses to PTH. NHERF1 permits selective activation of $G\alpha_q$, whereas NHERF2 attenuates PTH-stimulated $G\alpha_s$, while enhancing PTH-induced activation of $G\alpha_q$ and $G\alpha_i$. These findings explain why PTH stimulated $G\alpha_q$ and $G\alpha_i$ in C21 cells, which express both NHERF1 and NHERF2, but not in ROS 17/2.8 cells, which express neither. Consistent with this interpretation, PTH does not stimulate $[Ca^{2+}]_i$ in native ROS 17/2.8 cells (29). Upon transfection of NHERF1, however, PTH significantly increased $[Ca^{2+}]_i$. Notably, relatively high PTHR density is required for efficient activation of PLC, in contrast to receptor activation of adenylyl cyclase that occurs at physiologic receptor concentrations (52). This may contribute to the limited PLC activation in ROS 17/2.8 cells.

To demonstrate the generality of the effects of NHERF1 and NHERF2, we studied the PTH-dependent activation of heterotrimeric G proteins in several cell lines that have been used as models to analyze the heterogeneity of the responses to PTH. We chose PS120 fibroblasts, CHO-derived cell lines, and HEK-293 cells, all of which were transfected with either the WT-PTHR or a mutated form with an impaired PDZ-binding motif. Our results are summarized in Table 2. Several conclusions can be drawn from these results. For instance, the data clearly indicate that coupling of the PTHR to $G\alpha_i$ absolutely requires the expression of NHERF2. Furthermore, in the absence of NHERF1 and NHERF2, the receptor couples primarily to $G\alpha_s$. Finally, $G\alpha_q$ coupling is significantly increased by either NHERF1 or NHERF2.

These results are consistent with previous reports examining the downstream effects of PTH in various cell lines and now provide a mechanism to reconcile apparent discrepancies between different cells or cell lines. Furthermore, our findings provide a solid experimental framework to explain the complex spectrum of cellular responses to PTH. For example, in PS120 cells stably transfected with the PTHR, the expression of NHERF2 decreased cAMP responses and increased PLC-dependent effects (21). Our data show that this effect is due to increased $G\alpha_i$ and decreased $G\alpha_s$ activation in the presence of NHERF2. Likewise, HEK-293R robustly activate cAMP and Ca^{2+}-dependent responses. The present findings support the conclusion that this is due to NHERF1/NHERF2-dependent modulation of the pattern of G protein activation downstream of the PTHR in these cells.

FIGURE 5. **Effects of NHERF1 and NHERF2 on PTH-stimulated [^{35}S]GTPγS binding to Gα protein subunits in HEK-293R cell membranes.** *A*, GST-tagged C-terminal 22 amino acids of PTH1R (*PTHR-ctETVM*) and its mutant of PTHR-ctETVA were overlaid with His-tagged PDZ domain of NHERF1 or NHERF2 on nylon membranes as described under "Experimental Procedures." A representative overlay assay shows that PTH1R interacts with both PDZ domains of NHERF1 or NHERF2. *B*, equal amounts of membrane proteins (20 μg) from HEK-293R cells transiently transfected with HA-PTHR-ETVM or HA-PTHR-ETVA were immunoblotted (*IB*) with HA antibody. *C*, PTH-stimulated [^{35}S]GTPγs binding to $G\alpha_s$, $G\alpha_q$, or $G\alpha_i$ protein was measured in the cell membranes of HEK-293R cells transiently transfected with HA-PTHR-ETVM or HA-PTHR-ETVA. Data are summarized as the mean ± S.E. of four independent experiments. *, $p < 0.05$; **, $p < 0.01$ compared with PTHR-ETVM group. *D*, equal amounts of membrane proteins (20 μg) from HEK-293R cells transiently transfected with scrambled shRNA, NHERF1 shRNA (*shNHERF1*), or NHERF2 shRNA (*shNHERF2*) were immunoblotted with either NHERF1 or NHERF2 antibody. *E*, PTH-stimulated [^{35}S]GTPγs binding to $G\alpha_s$, $G\alpha_q$, or $G\alpha_i$ protein was measured in the cell membranes of HEK-293R cells transiently transfected with scrambled shRNA, shNHERF1 or shNHERF2. Data are summarized as the mean ± S.E. of four independent experiments. *, $p < 0.05$; **, $p < 0.01$, compared with scrambled plus PTH group. *F*, rescue experiments were performed by cotransfection with shNHERF1, shNHERF2, and plasmid constructs of WT-NHERF1, WT-NHERF2, or mutated NHERF1 and NHERF2 (resNHERF1 and resNHERF2) that are refractory to cleavage by their respective shRNA as described under "Experimental Procedures." PTH-stimulated [^{35}S]GTPγs binding to $G\alpha_s$, $G\alpha_q$, or $G\alpha_i$ protein was measured. Data are summarized as the mean ± S.E. of four independent experiments. **, $p < 0.01$, *versus* respective scrambled plus vector group. *G*, $G\alpha_i$ activation measured by real time FRET. FRET was performed on HEK-293 cells cotransfected with shNHERF1 or shNHERF2 and plasmid constructs of PTHR-ETVM, PTHR-ETVA, $^{YFP}G\alpha_i$ and bimolecular fluorescence complementation $\beta_1\gamma_2$ complexes as described under "Experimental Procedures." Data are summarized as the normalized FRET mean ± S.E. of three independent experiments.

Downloaded from www.jbc.org at Emory University, on December 17, 2010

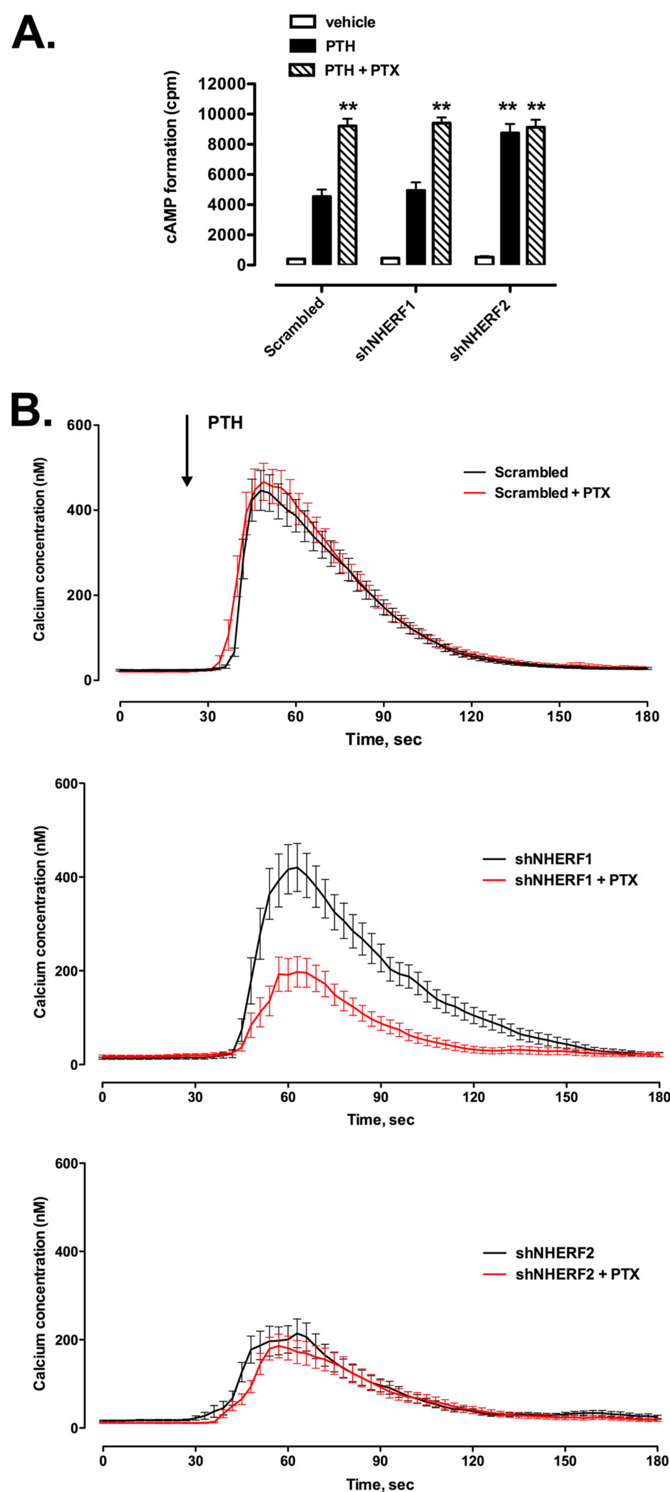

FIGURE 7. **Effects of NHERF1 and NHERF2 on PTH-stimulated adenylyl cyclase activity and $[Ca^{2+}]_i$.** *A*, effects of NHERF1 and NHERF2 on PTH-stimulated adenylyl cyclase activity. HEK-293R cells were transfected with scrambled shRNA, shNHERF1, or shNHERF2. Pertussis toxin (*PTX*) (100 ng/ml) was added for 16 h as indicated. Cells were treated with 100 nM PTH for 15 min, and cAMP accumulation was measured as described under "Experimental Procedures." Data are summarized as the mean ± S.E. of four independent experiments. **, $p < 0.01$ compared with scrambled shRNA plus PTH group. *B*, effects of NHERF1 and NHERF2 on PTH-induced $[Ca^{2+}]_i$. HEK-293R cells were treated as the same as *A*. PTH (100 nM)-stimulated $[Ca^{2+}]_i$ was measured as described under "Experimental Procedures." Data are summarized as the mean ± S.E. of three independent experiments. The effects of scrambled shRNA, shNHERF1, and shNHERF2 on $[Ca^{2+}]_i$ in the presence or absence of pertussis toxin were shown in *top, middle,* or *bottom panel*, respectively.

Despite the similarity of their PDZ domains and C-terminal ezrin-binding domain, NHERF1 and NHERF2 exhibit different affinities for PDZ-binding partners and GPCR signaling (20, 25, 53, 54). These results show that the PTHR binds preferentially to PDZ1 of NHERF1 and PDZ2 of NHERF2. Because binding to both NHERF proteins is mediated by the same C-terminal sequence, the PTH1R cannot simultaneously interact with NHERF1 and NHERF2. Thus, the relative levels of expression of NHERF1 and NHERF2 may influence the differential coupling of the PTHR to different downstream signaling pathways. Importantly, although it is clear that the expression of NHERF1 and NHERF2 influences PTHR signaling, some variations among cell lines have been reported, indicating the influence of additional factors in PTHR signaling. For instance, NHERF1 increases PTH-stimulated cAMP accumulation in ROS 17/2.8 cells (29) but decreases cAMP responses in OKH cells (30). Furthermore, PTH-stimulated cAMP production in wild-type and NHERF1-null proximal tubule cells was comparable (32, 33), as it is in CHO-N10-R3 cells in the presence or absence of NHERF1 (34). Our results indicate that NHERF1 has no effects on PTH-induced $G\alpha_s$ or $G\alpha_i$ activation; therefore, the different effects of NHERF1 on the production of cAMP by these cell lines are probably due to other factors that remain unidentified.

The effects of NHERF2 on adenylyl cyclase activation are somewhat less diverse. NHERF2 expression markedly inhibited adenylyl cyclase in PS120 cells transfected with the PTHR, a result that is consistent with the differential activation of $G\alpha_s$ and $G\alpha_i$ induced by NHERF2 expression (21). Both NHERF1 and NHERF2 increase PTH-stimulated PLC activity and intercellular calcium in PS120 cells, opossum kidney cells, or ROS 17/2.8 cells (21, 29–31). These findings are consistent with the model presented here. Both NHERF1 and NHERF2 increase the activation of PLCβ and the generation of intracellular Ca^{2+} transients. However, despite the similarities between NHERF1 and NHERF2, the coupling of the PTHR to calcium signaling is mediated by distinct mechanisms. In HEK-293R cells (which express both NHERF1 and NHERF2), the PTHR stimulates Ca^{2+} release by a mechanism that is insensitive to pertussis toxin. Thus, in the presence of both NHERF1 and NHERF2, a $G\alpha_q$-driven mechanism predominates. Knockdown of NHERF1 has no effect on the magnitude or duration of the Ca^{2+} transients but reveals significant sensitivity to pertussis toxin. This suggests that $G\alpha_i$ activation is important for Ca^{2+} release when only NHERF2 is present. Finally, knockdown of NHERF2 significantly reduces the magnitude of the Ca^{2+} release response, which in this case remains insensitive to pertussis toxin. A comparison of the magnitude of these responses suggests that NHERF2 is more efficient in the coupling of Ca^{2+} responses, which are mediated by the engagement of both G_q and G_i, whereas NHERF1 only supports G_q-mediated responses.

Because NHERF2 was reported to inhibit adenylyl cyclase by stimulating $G\alpha_i$ proteins in PS120 cells stably transfected with the PTHR or stably transfected with both the receptor and NHERF2 (21), we employed these cell models to investigate NHERF2 coupling of the PTHR to different $G\alpha$ protein subunits. The results show that NHERF2 significantly inhib-

Downloaded from www.jbc.org at Emory University, on December 17, 2010

TABLE 2
Summary of results with different cell lines

Cell line	NHERF expression	Treatment	Coupling
PS120-R	Neither	None	$G_s > G_q$; no G_i activation
		NHERF2	$G_q > G_i > G_s$
CHO-R	Neither	None	$G_s > G_q$; no G_i activation
		NHERF1	$G_q \cong G_s$; no G_i activation
		NHERF2	$G_q > G_i \cong G_s$
HEK-293-ETVM (WT-PTHR)	Both	None	$G_q > G_i \cong G_s$
		NHERF1 shRNA	$G_s \cong G_q \cong G_i$
		NHERF2 shRNA	$G_s > G_q$; no G_i activation
HEK-293-ETVA (PTHR with impaired PDZ binding)	Both	None	$G_s > G_q$; no G_i activation

ited PTH-stimulated $G\alpha_s$ activation but activated both $G\alpha_q$ and G_i, consistent with the reported NHERF2 regulation of PTHR second messenger signaling pathways (21). We further detailed the effect of NHERF1 on PTHR activation of $G\alpha$ subunits by using CHO cells stably transfected with PTHR (CHO-R cells), which do not constitutively express detectable NHERF1 or NHERF2. Consistent with the results with PS120-R-N2 cells, transient expression of NHERF1 did not affect PTH-induced activation of $G\alpha_s$ or $G\alpha_i$. However, expression of NHERF2 significantly inhibited PTH-induced $G\alpha_s$ but increased coupling of the PTHR to $G\alpha_q$ and $G\alpha_i$ proteins. Nonetheless, some inconsistencies regarding NHERF1 regulation of PTH-stimulated adenylyl cyclase activity have been reported (29, 30, 32–34). These differences may be ascribed to NHERF1 regulation of PTHR trafficking, cell specificity, or as yet unrecognized factors.

The precise mechanistic basis of the differential regulation of the G protein coupling of the PTHR by NHERF1 and NHERF2 remains to be explained. One plausible explanation is suggested by the data shown in Fig. 6. Both NHERF1 and NHERF2 coimmunoprecipitated with $G\alpha_q$, but only NHERF2 was able to pull down $G\alpha_i$. The specific regions of NHERF1 and NHERF2 that mediate these putative interactions remain unknown. The next question is as follows. How do the interactions with NHERF1 and NHERF2 with G proteins influence PTHR signaling? The simplest model involves the pre-formation of a multimeric complex involving the PTHR, NHERF1/NHERF2, and a heterotrimeric G protein. We propose that the formation of this complex, by bringing the receptor and the G protein into close proximity, facilitates G protein activation. Thus, NHERF1, which binds $G\alpha_q$, will promote G_q activation, and NHERF2, which binds $G\alpha_q$ and $G\alpha_i$, will enhance the activation of these two G proteins. The differential effects of NHERF1 and NHERF2 on G_s activation may be due to the different topology of the interactions of the two PDZ proteins with the PTHR. It is conceivable that NHERF1 binding to PTHR, which is mediated by the N-terminal PDZ1 domain, does not interfere with G_s binding. Conversely, NHERF2-PTHR interactions, which involve the central PDZ2 of NHERF2, may induce conformational changes that result in reduced affinity for $G\alpha_s$.

In summary, NHERF1 interacts with $G\alpha_q$ and increases PTH-stimulated PTHR coupling to $G\alpha_q$ but has no effect on $G\alpha_s$ or $G\alpha_i$. In contrast, NHERF2 interacts with both $G\alpha_q$ and $G\alpha_i$. Therefore, NHERF1 and NHERF2 control PTHR signaling by differential coupling of $G\alpha$ proteins to the PTHR. These novel findings explain the differences between NHERF1 and NHERF2 on downstream regulation of PTHR signaling.

Acknowledgment—We thank David Wheeler for constructive suggestions during the course of this study.

REFERENCES

1. Schwindinger, W. F., Fredericks, J., Watkins, L., Robinson, H., Bathon, J. M., Pines, M., Suva, L. J., and Levine, M. A. (1998) *Endocrine* **8,** 201–209
2. Offermanns, S., Iida-Klein, A., Segre, G. V., and Simon, M. I. (1996) *Mol. Endocrinol.* **10,** 566–574
3. Wu, S., Pirola, C. J., Green, J., Yamaguchi, D. T., Okano, K., Jueppner, H., Forrester, J. S., Fagin, J. A., and Clemens, T. L. (1993) *Endocrinology* **133,** 2437–2444
4. Maeda, S., Wu, S., Jüppner, H., Green, J., Aragay, A. M., Fagin, J. A., and Clemens, T. L. (1996) *Endocrinology* **137,** 3154–3162
5. Orloff, J. J., Kats, Y., Urena, P., Schipani, E., Vasavada, R. C., Philbrick, W. M., Behal, A., Abou-Samra, A. B., Segre, G. V., and Jüppner, H. (1995) *Endocrinology* **136,** 3016–3023
6. Whitfield, J. F., Chakravarthy, B. R., Durkin, J. P., Isaacs, R. J., Jouishomme, H., Sikorska, M., Williams, R. E., and Rixon, R. H. (1992) *J. Cell. Physiol.* **150,** 299–303
7. Rampe, D., Lacerda, A. E., Dage, R. C., and Brown, A. M. (1991) *Am. J. Physiol.* **261,** H1945–H1950
8. Schlüter, K. D., Weber, M., and Piper, H. M. (1995) *Biochem. J.* **310,** 439–444
9. Atkinson, M. J., Hesch, R. D., Cade, C., Wadwah, M., and Perris, A. D. (1987) *J. Bone Miner. Res.* **2,** 303–309
10. Klinger, M., Alexiewicz, J. M., Linker-Israeli, M., Pitts, T. O., Gaciong, Z., Fadda, G. Z., and Massry, S. G. (1990) *Kidney Int.* **37,** 1543–1551
11. Whitfield, J. F., MacManus, J. P., Youdale, T., and Franks, D. J. (1971) *J. Cell. Physiol.* **78,** 355–368
12. Abou-Samra, A. B., Jüppner, H., Force, T., Freeman, M. W., Kong, X. F., Schipani, E., Urena, P., Richards, J., Bonventre, J. V., Potts, J. T., Jr., Kronenberg, H. M., and Segre, G. V. (1992) *Proc. Natl. Acad. Sci. U.S.A.* **89,** 2732–2736
13. Hruska, K. A., Moskowitz, D., Esbrit, P., Civitelli, R., Westbrook, S., and Huskey, M. (1987) *J. Clin. Invest.* **79,** 230–239
14. Friedman, P. A., Coutermarsh, B. A., Kennedy, S. M., and Gesek, F. A. (1996) *Endocrinology* **137,** 13–20
15. Pines, M., Fukayama, S., Costas, K., Meurer, E., Goldsmith, P. K., Xu, X., Muallem, S., Behar, V., Chorev, M., Rosenblatt, M., Tashjian, A. H., Jr., and Suva, L. J. (1996) *Bone* **18,** 381–389
16. Iida-Klein, A., Guo, J., Xie, L. Y., Jüppner, H., Potts, J. T., Jr., Kronenberg, H. M., Bringhurst, F. R., Abou-Samra, A. B., and Segre, G. V. (1995) *J. Biol. Chem.* **270,** 8458–8465
17. Donowitz, M., Cha, B., Zachos, N. C., Brett, C. L., Sharma, A., Tse, C. M., and Li, X. (2005) *J. Physiol.* **567,** 3–11
18. Shenolikar, S., Voltz, J. W., Minkoff, C. M., Wade, J. B., and Weinman, E. J. (2002) *Proc. Natl. Acad. Sci. U.S.A.* **99,** 11470–11475
19. Bretscher, A., Edwards, K., and Fehon, R. G. (2002) *Nat. Rev. Mol. Cell Biol.* **3,** 586–599
20. Shenolikar, S., Voltz, J. W., Cunningham, R., and Weinman, E. J. (2004)

Downloaded from www.jbc.org at Emory University, on December 17, 2010

Physiology **19,** 362–369
21. Mahon, M. J., Donowitz, M., Yun, C. C., and Segre, G. V. (2002) *Nature* **417,** 858–861
22. Paquet, M., Asay, M. J., Fam, S. R., Inuzuka, H., Castleberry, A. M., Oller, H., Smith, Y., Yun, C. C., Traynelis, S. F., and Hall, R. A. (2006) *J. Biol. Chem.* **281,** 29949–29961
23. Kanai, F., Marignani, P. A., Sarbassova, D., Yagi, R., Hall, R. A., Donowitz, M., Hisaminato, A., Fujiwara, T., Ito, Y., Cantley, L. C., and Yaffe, M. B. (2000) *EMBO J.* **19,** 6778–6791
24. DeMarco, S. J., Chicka, M. C., and Strehler, E. E. (2002) *J. Biol. Chem.* **277,** 10506–10511
25. Lin, S., Yeruva, S., He, P., Singh, A. K., Zhang, H., Chen, M., Lamprecht, G., de Jonge, H. R., Tse, M., Donowitz, M., Hogema, B. M., Chun, J., Seidler, U., and Yun, C. C. (2010) *Gastroenterology* **138,** 649–658
26. Hwang, J. I., Heo, K., Shin, K. J., Kim, E., Yun, C., Ryu, S. H., Shin, H. S., and Suh, P. G. (2000) *J. Biol. Chem.* **275,** 16632–16637
27. Kim, J. H., Lee-Kwon, W., Park, J. B., Ryu, S. H., Yun, C. H., and Donowitz, M. (2002) *J. Biol. Chem.* **277,** 23714–23724
28. Oh, Y. S., Jo, N. W., Choi, J. W., Kim, H. S., Seo, S. W., Kang, K. O., Hwang, J. I., Heo, K., Kim, S. H., Kim, Y. H., Kim, I. H., Kim, J. H., Banno, Y., Ryu, S. H., and Suh, P. G. (2004) *Mol. Cell. Biol.* **24,** 5069–5079
29. Wheeler, D., Garrido, J. L., Bisello, A., Kim, Y. K., Friedman, P. A., and Romero, G. (2008) *Mol. Endocrinol.* **22,** 1163–1170
30. Mahon, M. J., Cole, J. A., Lederer, E. D., and Segre, G. V. (2003) *Mol. Endocrinol.* **17,** 2355–2364
31. Mahon, M. J., and Segre, G. V. (2004) *J. Biol. Chem.* **279,** 23550–23558
32. Cunningham, R., Steplock, D., Wang, F., Huang, H., E, X., Shenolikar, S., and Weinman, E. J. (2004) *J. Biol. Chem.* **279,** 37815–37821
33. Cunningham, R., E, X., Steplock, D., Shenolikar, S., and Weinman, E. J. (2005) *Am. J. Physiol. Renal Physiol* **289,** F933–F938
34. Wang, B., Bisello, A., Yang, Y., Romero, G. G., and Friedman, P. A. (2007) *J. Biol. Chem.* **282,** 36214–36222
35. Rochdi, M. D., Watier, V., La Madeleine, C., Nakata, H., Kozasa, T., and Parent, J. L. (2002) *J. Biol. Chem.* **277,** 40751–40759
36. Lee-Kwon, W., Kim, J. H., Choi, J. W., Kawano, K., Cha, B., Dartt, D. A., Zoukhri, D., and Donowitz, M. (2003) *Am. J. Physiol. Cell. Physiol* **285,** C1527–C1536
37. Kunkel, M. T., Garcia, E. L., Kajimoto, T., Hall, R. A., and Newton, A. C. (2009) *J. Biol. Chem.* **284,** 24653–24661
38. Hynes, T. R., Tang, L., Mervine, S. M., Sabo, J. L., Yost, E. A., Devreotes, P. N., and Berlot, C. H. (2004) *J. Biol. Chem.* **279,** 30279–30286
39. Wang, B., Yang, Y., and Friedman, P. A. (2008) *Mol. Biol. Cell* **19,** 1637–1645
40. Akam, E. C., Challiss, R. A., and Nahorski, S. R. (2001) *Br J. Pharmacol.* **132,** 950–958
41. Wang, B., Yang, Y., Abou-Samra, A. B., and Friedman, P. A. (2009) *Mol. Pharmacol.* **75,** 1189–1197
42. He, J., Bellini, M., Inuzuka, H., Xu, J., Xiong, Y., Yang, X., Castleberry, A. M., and Hall, R. A. (2006) *J. Biol. Chem.* **281,** 2820–2827
43. Bünemann, M., Frank, M., and Lohse, M. J. (2003) *Proc. Natl. Acad. Sci. U.S.A.* **100,** 16077–16082
44. Frank, M., Thümer, L., Lohse, M. J., and Bünemann, M. (2005) *J. Biol. Chem.* **280,** 24584–24590
45. Vilardaga, J. P., Nikolaev, V. O., Lorenz, K., Ferrandon, S., Zhuang, Z., and Lohse, M. J. (2008) *Nat. Chem. Biol.* **4,** 126–131
46. Woodruff, M. L., Sampath, A. P., Matthews, H. R., Krasnoperova, N. V., Lem, J., and Fain, G. L. (2002) *J. Physiol.* **542,** 843–854
47. Ahn, W., Kim, K. H., Lee, J. A., Kim, J. Y., Choi, J. Y., Moe, O. W., Milgram, S. L., Muallem, S., and Lee, M. G. (2001) *J. Biol. Chem.* **276,** 17236–17243
48. Sun, C., and Mierke, D. F. (2005) *J. Pept. Res.* **65,** 411–417
49. Sneddon, W. B., Syme, C. A., Bisello, A., Magyar, C. E., Rochdi, M. D., Parent, J. L., Weinman, E. J., Abou-Samra, A. B., and Friedman, P. A. (2003) *J. Biol. Chem.* **278,** 43787–43796
50. Mahon, M. J., Bonacci, T. M., Divieti, P., and Smrcka, A. V. (2006) *Mol. Endocrinol.* **20,** 136–146
51. Yamamoto, I., Shigeno, C., Potts, J. T., Jr., and Segre, G. V. (1988) *Endocrinology* **122,** 1208–1217
52. Bringhurst, F. R., Juppner, H., Guo, J., Urena, P., Potts, J. T., Jr., Kronenberg, H. M., Abou-Samra, A. B., and Segre, G. V. (1993) *Endocrinology* **132,** 2090–2098
53. Weinman, E. J., Hall, R. A., Friedman, P. A., Liu-Chen, L. Y., and Shenolikar, S. (2006) *Annu. Rev. Physiol.* **68,** 491–505
54. Lau, A. G., and Hall, R. A. (2001) *Biochemistry* **40,** 8572–8580
55. Tawfeek, H. A., Qian, F., and Abou-Samra, A. B. (2002) *Mol. Endocrinol.* **16,** 1–13

Downloaded from www.jbc.org at Emory University, on December 17, 2010